Power Converters for Power-Ultrasonic Transducers

Ying Wang
University of Bath
yw244@bath.ac.uk

Mike Draper
Sonic Systems Ltd
mike.draper
@sonicsystems.co.uk

Simon Denley
Sonic Systems Ltd
simondenley
@sonicsystems.co.uk

Francis Robinson
University of Bath
eesfvpr@bath.ac.uk

Peter Shepherd
University of Bath
eesprs@bath.ac.uk

***Abstract*-High-performance power-converters in the form of single-tone class-D amplifiers are required to drive power-ultrasonic transducers in industrial applications. These must produce low-distortion, variable-frequency, and variable-amplitude sinusoidal currents to efficiently drive the piezoelectric cell and horn of transducers, and thereby vibrate material-processing stages. A resonant-tracking control strategy is generally used to efficiently couple and regulate output power delivery at a high-Q probe-system resonant mode. This paper reviews a number of power-converter control options suitable for such probe drivers, including quasi-squarewave (QS), naturally sampling pulse width modulation (PWM) and programmed PWM (PPWM). Typical output-waveform quality and the PSPICE models of the power-converter and piezoelectric transducer developed to assess and compare methods are presented.**

***Index Terms*—Class-D driver, piezoelectric transducer driver, power-ultrasonic system, programmed PWM, PWM, quasi-squarewave, ultrasonic transducer PSPICE model.**

I. INTRODUCTION

Power ultrasonics is a technology for exciting and maintaining mechanical vibration or resonance, most commonly between 20kHz to 120kHz, in industrial material or chemical processing equipment. The acoustic power is usually generated using one or more piezoelectric transducers driven by a resonant-tracking single-tone electronic power amplifier. The power level required by different processes varies. In some, such as medical surgery, a few Watts only is required, whereas others, such as ultrasonic cleaning bath, may require up to several kilowatts [1].

Fig. 1 shows a typical power ultrasonic system, comprising the ultrasonic transducer and its generator or driver. The ultrasonic generator is usually powered from a mains supply and delivers approximately sinusoidal output current to different transducers. Such a generator usually contains automatic frequency and amplitude control loops, which are used to ensure that the ultrasonic power to the acoustic load is generated at a desired level at the correct resonant frequency for the processing equipment and material involved [2][3].

A number of power-converter control options have been identified and analyzed, including quasi-squarewave (QS), sine-wave pulse width modulation (PWM) and programmed PWM (PPWM) as part of a project to design and develop an efficient, easily controlled generator system with a power-factor-corrected input stage for direct-off-line connection.

This less widely known application of variable-frequency power conversion will be of particular interest to others working on resonant-load driving, induction heating and other AC-supply frequency-tracking applications, as well as being of interest to the power-converter and power-amplifier research and development community generally.

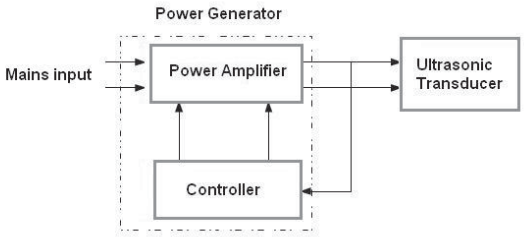

Fig.1 Typical layout of a power ultrasonic system.

II. EXISTING CONTROL LOOPS

Fig.2 shows the two main control loops, namely, current feedback loop and frequency control loop, typically found in existing system [4] [5]. The DC-DC converter draws its input via a mains rectifier and its output level is regulated to satisfy the load power level required. Its output serves as the bus voltage for the following DC-AC inverter which operates at the probe resonant frequency, tracked by the phase lock loop (PLL) [2][3][6]-[9]. The sensed load current is obtained from a fraction of the secondary winding of the output transformer and used for both current and frequency control.

Using two separate power converters for amplitude and frequency control results in greater overall conversion losses, component cost and system weight and volume than a modern single-stage inverter topology, which enables both amplitude and frequency control. To implement this idea, three possible solutions have been investigated.

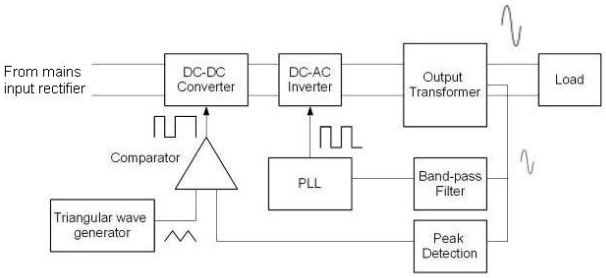

Fig.2 Two main control loops of existing power converter.

ISBN 978-3-8007-3402-3

III. POWER CONVERTER OPTIONS

A. *Quasi-squarewave*

Using the full-bridge topology, shown in Fig.3 [10], we can derive the waveform patterns as illustrated in Fig.4 when quasi-squarewave scheme is applied. Both the pulse width and period of the waveform can be varied according to the instantaneous power required and its resonant frequency. Therefore in theory a constant bus voltage can be used for the inverter stage in this case.

Fourier analysis can be used to quantify the amplitude variation of the V_{AB} fundamental and harmonic components. To do this, the time axis is changed to a radian-angle axis as shown in Fig.5, with the time-zero adjusted to make V_{AB} of half-wave symmetry having only odd harmonics. The delay T_d is represented by 2α.

The waveform shows an odd form function which has no cosine components. It does not contain DC value due to its zero average value. The magnitude of the fundamental and harmonic components can be calculated as:

$$V_h = \frac{1}{\pi}\int_0^{2\pi} v_{AB}(\omega t)\sin(h\omega t)\,d\omega t \qquad (1)$$

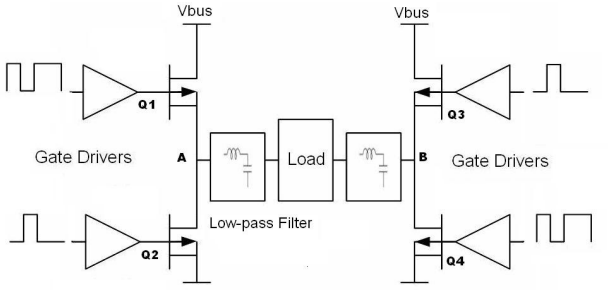

Fig.3 Full-bridge topology.

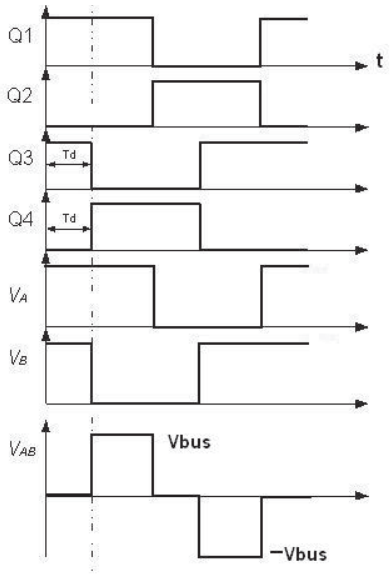

Fig.4 Quasi-squarewave switching and output waveforms.

where h=1,3,5… is the order of harmonic. When α is the switching angle and V_{BUS} is the bus voltage, (1) can be calculated as:

$$V_h = \frac{4V_{BUS}}{h\pi}\cos(h\alpha)$$

and the amplitude of fundamental can be derived as

$$V_1 = \frac{4V_{BUS}}{\pi}\cos(\alpha)$$

whose value decreases from 1, when α is $0°$, to 0 when α is $90°$ [12]. Fig.5 shows the normalized amplitude of output voltage harmonics when QS is used as the full-bridge drive signal.

B. *Sinewave-PWM*

The second possible approach is to implement PWM of higher switching frequencies, i.e. several times the resonant frequency, in order to generate an output current with a better sinewave approximation to reduce harmonics. Again based on the full-bridge structure in Fig.3, Fig.6 shows typical waveforms of a sinewave-PWM switching scheme with 12 pulses each base-band period [11].

However since a typical ultrasonic system operates from 20 to 120kHz, using excessive high switching frequency, i.e. greater than 1MHz, will increase switching loss and lower system efficiency. Therefore only PWM with up to 5 pulses is to be considered in this case.

Modulation index, m_a, is the amount of full-scale signal that can be output from the PWM amplifier. It is given in (2) as the amplitude ratio of the input signal V_{IN} to the carrier signal V_C [13]:

$$m_a = \frac{V_{IN}}{V_C} \qquad (2)$$

.

C. *Programmed-PWM*

The concept of PPWM was first introduced in 1973 as a scheme to perform effective harmonic elimination by inserting an even number of symmetric zero-voltage gaps into each positive and negative section of the squarewave [14][15]. Fig.7 shows a PPWM waveform with 4 gaps inserted (number of switching angles N=5) in each half waveform.

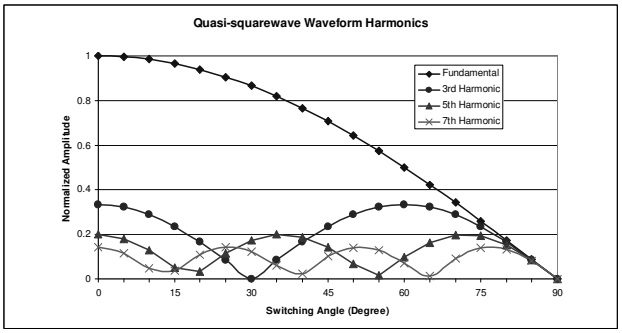

Fig.5 Normalized amplitude of voltage harmonics when using QS switching.

ISBN 978-3-8007-3402-3

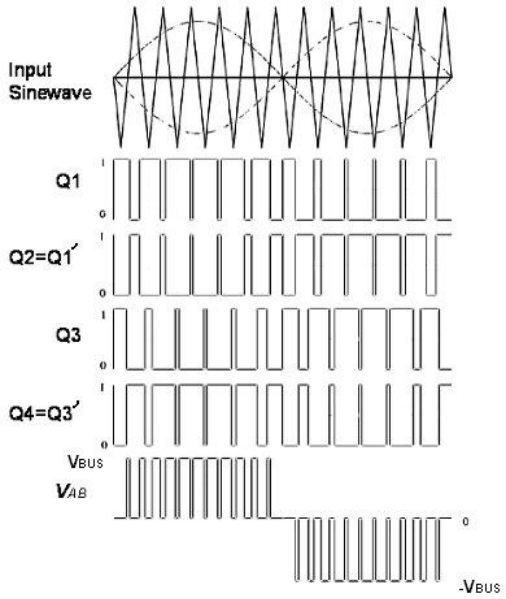

Fig.6 Generation of PWM, switching and output waveforms.

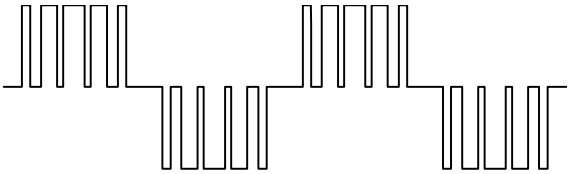

Fig.7 N=5 PPWM waveform v_{PPWM}.

Again based on Fourier series, the PPWM waveform of unit amplitude can be represented as:

$$v_{PPWM}(\omega t)=\sum_{h=1}^{\infty}\left[a_h\sin(h\omega t)+b_h\cos(h\omega t)\right]$$

and due to its quarter-wave symmetry, the Fourier coefficients are given by:

$$\begin{cases} a_h=\dfrac{4}{h\pi}\displaystyle\sum_{k=1}^{N}(-1)^{k+1}\cos(h\alpha_k) & h-odd \\ a_h=0 & h-even \\ b_h=0 & h=1,2,\cdots N \end{cases}$$

where switching angles $0<\alpha_1<\alpha_2<.....<\alpha_N<\dfrac{\pi}{2}$.

The magnitude of the fundamental and harmonic components can be calculated by:

$$V_h=\frac{4}{h\pi}\sum_{k=1}^{N}(-1)^{k+1}\cos(h\alpha_k)$$

where

$$\begin{cases} V_1=\dfrac{4}{\pi}\displaystyle\sum_{k=1}^{N}(-1)^{k+1}\cos(\alpha_k)=m_a \\ V_3=\dfrac{4}{3\pi}\displaystyle\sum_{k=1}^{N}(-1)^{k+1}\cos(3\alpha_k)=0 \\ \vdots \\ V_{2N-1}=\dfrac{4}{(2N-1)\pi}\displaystyle\sum_{k=1}^{N}(-1)^{k+1}\cos((2N-1)\alpha_k)=0 \end{cases} \quad (4)$$

(4) represents that the PPWM is designed to eliminate 3rd, 5th … (2*N*-1)th-order harmonics. Thus *N* equations and *N* variables, $\alpha_1 \ldots \alpha_N$, need to be solved [16]-[18].

For example, switching angles for PPWM of *N*=5 when modulation index, m_a, from 0 to 1 are shown in Fig.8 [17]. In theory such a PPWM scheme is used to eliminate the 3rd, 5th, 7th and 9th-order harmonics.

IV. SIMULATION AND RESULTS

A. *Piezoelectric transducer modeling by PSPICE*

Modelling and simulation of Ultrasonic transducers could help to obtain a basic knowledge about characteristics of real transducers such as resonant frequencies and impedance values before fabrication [19]. It is also very useful for the development of its power generator. Fig.9 shows a PSpice model of an existing sandwiched transducer resonating around 35kHz.

Transmission lines T_BACK, T_CERAMIC, T_FRONT and T_BOLT represent the transducer back mass, piezoelectric ceramics, front mass and bolt respectively. Co is the static capacitance. Detailed information on the structure and parameter calculations of PSpice transducer model using transmission line and controlled source is beyond the scope of this paper but can be found in [20]-[21].

Fig.10 compares the real and imaginary parts of admittance as well as the resonant frequencies in simulation and experimental environments. These two sets of measurements have similar shape in waveforms. The difference of 0.3 kHz in resonant frequencies, less than 1%, is due to the approximation of transducer physical dimensions, e.g. layers of front masses, which vary in size, have been simplified to one transmission line model with constant diameter and acoustic velocity.

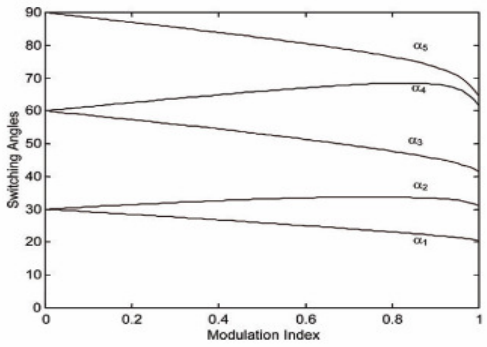

Fig.8 Switching angles for PPWM *N*=5.

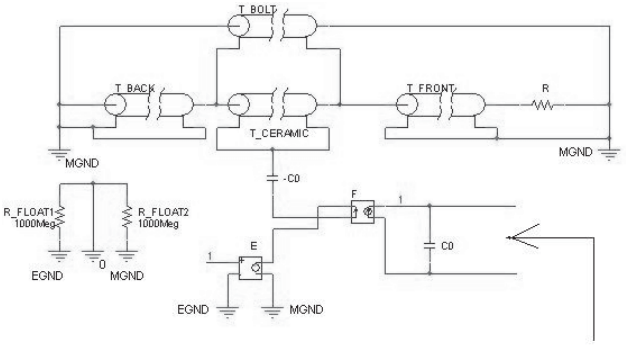

Fig.9 PSpice transmission-line model of a 35kHz Ultrasonic transducer.

The waveform inconsistency occurs at the resonance in Fig.10(b) was caused by the dramatic change in transducer admittance values around resonant frequency where there is frequency resolution limitation with the measuring equipment available.

Another advantage of using such transmission-model model is that it comes with harmonics due to the characteristics of transmission line, which makes it a better approximation to the real transducer and is ideal to evaluate the power converter performance in harmonic elimination. Fig.11 shows its fundamental, 3rd and 5th harmonics.

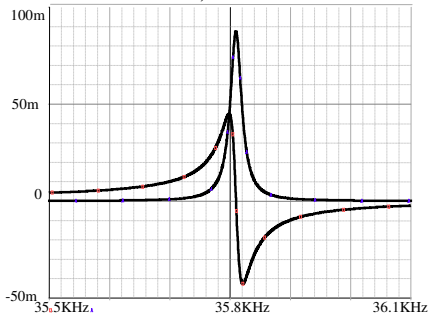

(a)

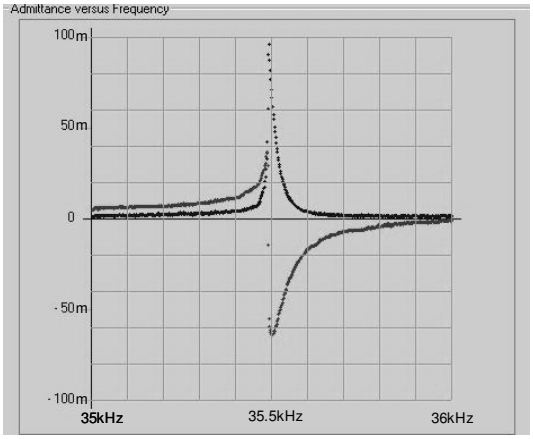

(b)

Fig.10 Transducer admittance plots around resonant frequency (a) PSpice simulation; (b) real measurement..

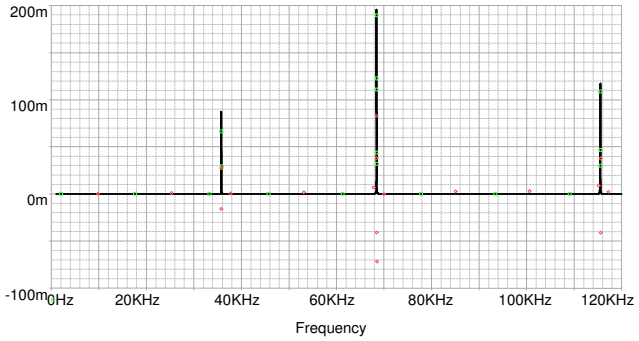

Fig.11 Real part of the admittance showing fundamental, 3rd and 5th harmonics of the transducer model.

B. *Switching simulation with matching inductor*

Fig. 12 illustrates the simulation circuits for evaluating the performance of different switching schemes introduced in Section III. L_MATCHING is the matching inductor whose value is calculated based on [22].

The two voltage controlled voltage sources, labelled E, model the function of the full-bridge inverter. The gain is chosen to be 100, representing a 100V DC bus voltage since the input signal ranges from 0 to 1.

C. *Results and conclusions*

Firstly we compare the performance of harmonic elimination by delivering 80% of the full-scale output power, m_a=0.8, using different switching schemes. Fig.13 shows the output voltages in the top window and load current in the bottom.

It can be seen that when N=3, PPWM option has no 3rd and 5th harmonics and 5-pulse PPWM successfully eliminates harmonics up to the 9th order. However both QS and PWM result in the existence of such lower-order harmonics.

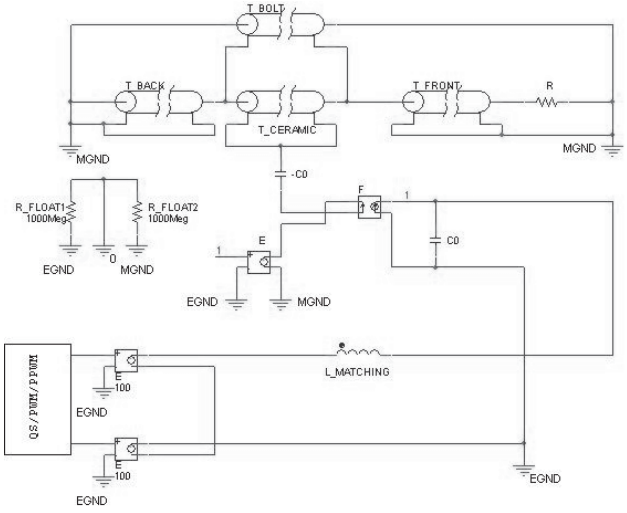

Fig.12 Simulation circuit for switching scheme evaluation.

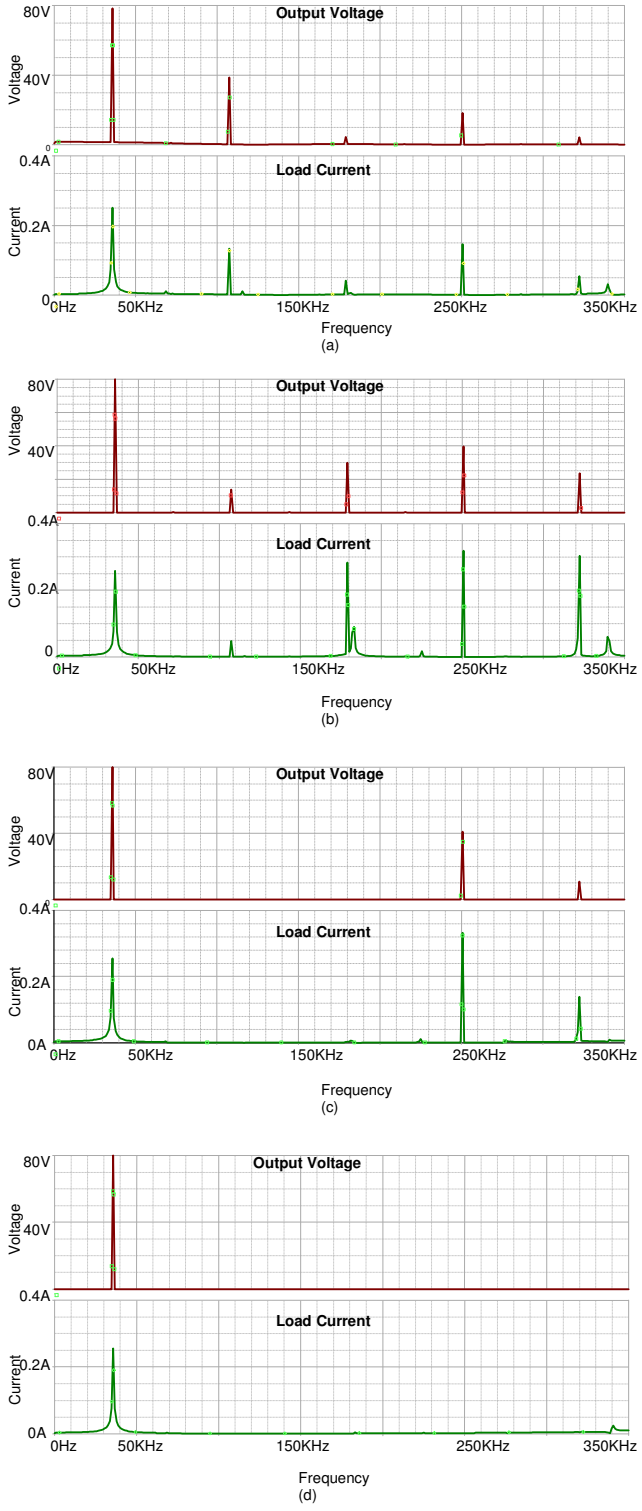

Fig.13 Performance of harmonic elimination with different switching schemes when m_a=0.8 (a) QS; (b) N=3 PWM; (c) N=3 PPWM; (d) N=5 PPWM.

A comprehensive comparison is given in Fig.14 and 15. Fig.14 describes the normalized load current amplitudes of fundamental and lower-order harmonics with regard to different switching angles when using quasi-squarewave switching scheme, which can be viewed in conjunction with its output voltage in Fig.5. Normalized amplitudes of fundamental, 3rd, 5th and 7th harmonic currents are shown in Fig.15 when driving with 3 and 5 pulses PWM and PPWM respectively.

Both PWM and PPWM give linear modulation when m_a is in the range of 0 and 1. Fig.14 also indicates that no matter what switching scheme is applied, the more pulses the system uses the better sinewave approximation it achieves, thus the smaller its lower-order harmonics become. Therefore the switching frequencies need to be optimized to balance the trade-offs between harmonics and switching losses.

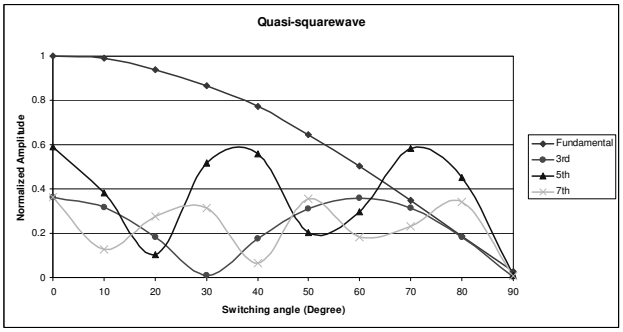

Fig.14 Normalized amplitude of output harmonics when QS is used.

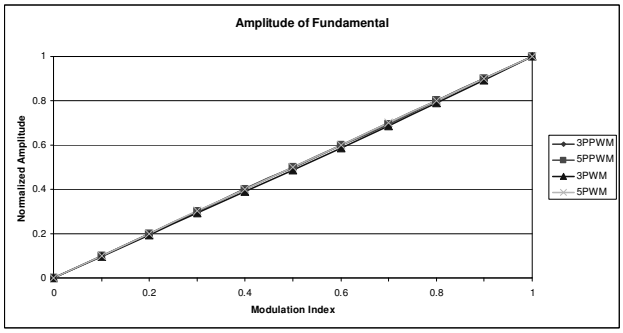

(a)

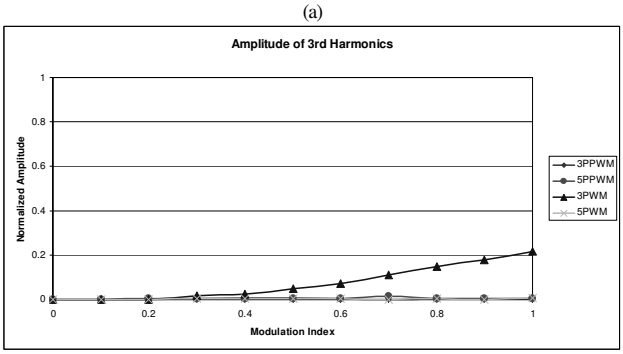

(b)

ISBN 978-3-8007-3402-3

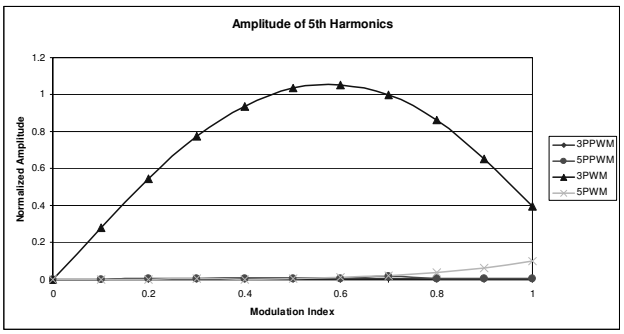

(c)

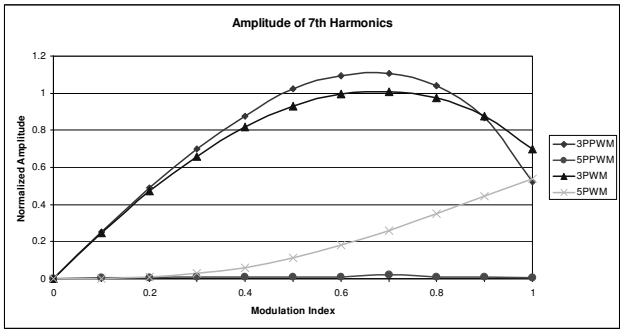

(d)

Fig.15 Normalized amplitude of output harmonics (a) fundamental; (b) 3rd harmonic; (c) 5th Harmonic; (d) 7th Harmonics.

In order to eliminate up to the 5th harmonics, 5 pulses are required for PWM whilst by using PPWM we can decrease the pulse number to 3. Using fewer pulse numbers results in lower switching losses therefore PPWM can be seen as a more effective and efficient method compared with the other two options.

V. CONCLUSIONS

Three possible solutions for power conversion, including QS, PWM and PPWM, have been identified and investigated in this paper for piezoelectric transducers. Results have shown that PPWM gives the best performance in terms of both effective harmonic elimination and low switching loss. A digital PPWM generator is to be made for driving ultrasonic transducers in the practical environment. Results are to be compared with simulation waveforms to further prove the suitability of PPWM method in power ultrasonic converters and its advantages over other switching schemes.

REFERENCES

[1] J.P. Perkins, "An outline of power ultrasonics," *OEM Design*, London: Mercury House, 1972.

[2] J. Ishikawa, Y. Mizutani, T. Suzuki, H. Ikeda and H. Yoshida, "High-frequency drive-power and frequency control for ultrasonic transducer operating at 3MHz," *Conference Record of the 1997 IEEE Industry Applications Conference Thirty-Second IAS Annual Meeting*, Vol. 2, pp. 900-905, 1997.

[3] V.N. Khmelev, R.V. Barsokov, S.N. Tsyganok, and M.V. Khmelev, "Phase lock system of ultrasonic electronic generators," *7th International Siberian Workshop and Tutorials EDM, (Session VI),* pp. 229-231, 2006.

[4] S. Ben-yaakov, E. Rozanov, T. Wasserman, T. Rafaeli, L. Shiv and G. Ivensky, "A resonant driver for a piezoelectric motor with single transistor direction switches," *15th Annual IEEE Applied Power Electronics Conference and Exposition,* vol.2, pp.1037-1043, 2000.

[5] L. Svilainis and G. Motiejunas, "Power amplifier for ultrasonic transducer excitation," *ULTRAGASRSAS*, Vol. 58(1), pp.30-36, 2006.

[6] L.J. Smith, "Use of phase-locked-loop control for driving ultrasonic transducer," *NASA Technical Note*, D-3567, 1966.

[7] Y. Mizutani, T. Suzuki, H. Ikeda and H. Yoshida, "Automatic frequency control for maximizing RF power fed to ultrasonic transducer operating at 1 MHz," *Conference Record of the 1996 IEEE Industry Applications Conference Thirty-First IAS Annual Meeting*, Vol. 3, pp. 1585-1588, 1996.

[8] Y. Peng, J. Xu, and Y. Li, "Modeling and simulation of an improved PLL-controlled circuit for series resonant inverter," *International Conference on Electrical Machines and Systems*, pp. 1786-1788, 2008.

[9] B. Mortimer, T. Du Bruyn, J. Davies and J. Tapson, "High power resonant tracking amplifier using admittance locking," *Ultrasonics*, Vol. 39 (4), pp. 257-261, 2001.

[10] J.S. Chang, M.T. Tan, Z. Cheng and Y.C. Tong, "Analysis and design of power efficient class d amplifier output stage," *IEEE Trans on Circuit and Systems I: Fundamental Theory and Applications*, Vol. 47(6), pp. 897-902, 2000.

[11] N. Mohan, T.M. Undeland and W.P. Robbins, *Power Electronics: Converters, Applications and Design.* 3rd ed. Hoboken: Wiley, 2003.

[12] Grant, D.A., Houldwirth, J.A. and Lower, K.N., A New High-Quality PWM AC Drive. *IEEE Transactions on Industry Applications*, 19 (2), pp. 211-216, 1983.

[13] D.G. Holmes and T.A Lipo, *Pulse Width Modulation for Power Converters: Principles and Practice*. Wiley-IEEE Press, 2003.

[14] H.S. Patel and R.G. Hoft, "Generalized techniques of harmonic elimination and voltage control in thyristor inverter: part I- harmonic elimination," *IEEE Trans. on Industrial Application*, IA-9(3), pp.310-317, 1973.

[15] P.N. Enjeti, P.D. Ziogas and J.F. Lindsay, "Programmed PWM techniques to eliminate harmonics: a critical evaluation," *IEEE Transactions on Industry Application*, Vol.26 (2), pp.302-316, 1990.

[16] P.N. Enjeti and J.F. Lindsay, "Solving nonlinear equations of harmonic elimination PWM in power control," *IEEE Electronics Letters*, Vol. 23(12), pp.656-657, 1987.

[17] J.W. Chen and T.J. Liang, "A novel algorithm in solving nonlinear equation for programmed PWM inverter to eliminate harmonics," *23rd Annual Conference of IEEE Industrial Electronics Society (IECON 97),* 2, pp.698-703, 1997.

[18] L. Li, D. Czarkowski, Y. Liu and P. Pillay, "Multilevel selective harmonic elimination PWM technique in series-connected voltage inverters," *IEEE Transactions on Industry Applications*, Vol.36 (1), pp.160-170, 2000.

[19] J. Deventer, T. Lofqvist and J. Delsing, "PSpice Simulation of Ultrasonic Systems," *IEEE Transactions on Ultrasonics*, Vol.47 (4), pp.1014-1024, 2000.

[20] W. M. Leach, Jr., "Controlled-source analogous circuits and SPICE models for piezoelectric transducers," *IEEE Trans. Ultrason., Ferroelect., Freq. Contr.*, vol. 41, pp. 60–66, 1994.

[21] E. Maione, P. Tortoli, G. Lypacewicz, A. Nowicki and J.M. Reid, "PSpice modeling of ultrasound transducers: comparison of software models to experiment," *IEEE Trans. Ultrason., Ferroelect. Freq. Contr.*, vol.46, no.2, 1999.

[22] C.M. Van Der Burgt and H.S.J Pijls, "Motional positive feedback systems for ultrasonic power generators," *IEEE Transactions on Ultrasonics Engineering,* Vol.10 (1), pp.2-19, 1963.

ISBN 978-3-8007-3402-3